

## ANALYTICAL AND NUMERICAL SOLUTION FOR PERISTALTIC MOTION OF A CASSON FLUID CONSIDERING SLIP EFFECTS

<sup>1</sup>Dr. UDAY RAJ SINGH, <sup>2</sup>UMA SHANKER

<sup>1</sup>Associate Professor, Department of Mathematics, C.L. Jain (P.G.)  
College, Firozabad, U.P., Affiliated to Dr. Bhimrao Ambedker University, Agra (India)

<sup>2</sup>Research Scholar, Department of Mathematics, C.L. Jain (P.G.)  
College, Firozabad, U.P., Affiliated to Dr. Bhimrao Ambedker University, Agra (India)

Chapter ID: NSP/ICAAR-2023/A-25

### ABSTRACT

Casson fluid, which is expected to flow in a non-uniform inclined channel, has been modeled to exhibit peristaltic motion. The channel wall should be lined with a non-erodible porous substance. It is assumed that the flow is taking place within a wave frame of reference and is travelling at the same velocity as a sinusoidal wave. It is possible to get analytical solutions for the variables of velocity, stream function, pressure gradient, pressure differential, and frictional force. Using MATLAB, graphs are displayed to illustrate the results of the velocity, stream function, and pressure gradient in relation to the axial displacement. As the Darcy number rises, it is observed that the velocity field, the velocity in the plug flow region, and the stream function all rises as well. It has also been observed that the same performance measurements get worse when the slip effect and porous thickening get worse. It can be observed that the pressure gradient lowers when the Darcy number, slip effect, porous thickening, and yield stress all increase, however the pressure gradient increases when the angle of inclination increases.

**Keyword:** Casson fluid, Reynolds number, sinusoidal wave, wave speed, wavelength

### INTRODUCTION

Many biological systems and industrial pumps rely on peristaltic motion to move fluids. As the wave moves through the length of a channel filled with fluid, the fluid is agitated and carried in the same direction.

Assuming the Poiseuille rule holds locally, Rubinow and Keller (1972) demonstrated that the tube's diameter could be regulated by strain in the walls and the transmural weight difference. Raju and Devanathan (1972) developed the first quantitative method for analysing peristaltic motion in fluids that are not Newtonian. Hummady and Abdulhadi looked at the effects of slip and heat transfer on peristaltic motion in MHD using a non-Newtonian fluid moving through a porous material in 2014. In 2015, Akbar and Butt studied the effect of heat transfer on the peristaltic transport of a Herschel-Bulkley fluid in a non-uniform channel. Ali et al. (2016) use the homotopy perturbation method to investigate the peristaltic flow of a hyperbolic tangent fluid through a three-dimensional non-uniform channel with flexible walls, and they find that the velocity is highest in the middle of the channel and lowest towards its walls. Pressure difference is shown to grow with porosity thickening while frictional force is reduced, as observed by Sankad and Patil (2016). Upon looking at all of the characteristics, they found that the pressure difference behaved in the opposite way to the frictional force. Gudekote and Choudhari (2018)

explored the interplay between slip and inclination for peristaltic transport of Casson fluid in a flexible tube with porous walls. Hasan et al. (2019) investigated peristaltic flow of a non-Newtonian fluid in an asymmetric porous channel using a slip parameter and a magnetic field. Laidoudi and Makinde (2022) numerical investigation of buoyancy effects in a hollow with two hot cylinders reveals some interesting phenomena. Using a non-Newtonian liquid that meets the Bingham plastic condition, Singh and Shanker (2022) studied the flow caused by the sinusoidal non-uniform peristaltic motion of the cylinder divider. Majeed et al. (2023) conducted a comprehensive study of the heat and mass transport properties of a Casson fluid flowing past a cylinder in a wavy channel. Heat and mass transport characteristics of a Casson fluid flow past a cylinder in a wavy channel were extensively analyzed by Majeed et al. (2023).

### FORMULATION OF THE PROBLEM

Consider the Casson fluid moving in a channel lined with an impermeable porous material and having a width of  $m$ . A peristaltic wave travelling along the channel's flexible wall at a speed  $c$  is applied with an amplitude  $l$  and a wave length of  $\lambda$ . The considered channel is not horizontal and is slanted at an angle  $\varphi$ .

For this discussion, just half of the channel width is taken into account. Near the plug flow boundary Between the plugs, or in the plug flow region  $y = 0$  and  $y = y_0$  when  $\tau_{yx} \leq \tau_0$  in addition to the area between  $y = y_0$  and  $y = K$  when  $\tau_{yx} \geq \tau_0$ .

Calculating the wall's distortion requires only knowing

$$Y = K = m + l \sin \frac{2\pi}{\lambda} (X - ct) \tag{1}$$

Where  $m = a + bx$ , where  $a$  indicates the channel's inlet width in half. Furthermore, it is assumed that the channel length is a whole number multiple of the wavelength  $\lambda$  Because the pressure gradient between the beginning and end of the channel is constant, we have steady flow in the wave frame  $(x, y)$ , conforming to the speed  $c$  exterior to the confines of the laboratory  $(X, Y)$ . The flow is chaotic even in the well constructed  $(X, Y)$ , laboratory frame. Yet, when viewed from a wave frame  $(x, y)$ , the boundary shape remains unchanged despite the change in the coordinate framework's propagation velocity  $c$ .

#### Here's how these two wave frames relate to one another:

$$x = X - ct, y = Y, u = U - c, v = V \tag{2}$$

where  $U, V$ , and  $u, v$  represent the laboratory frame and wave frame velocity components, respectively.

According to the available data, the Reynolds number of the flow is low in many physiological contexts. Assuming inertially free flow, the wavelength is unbounded. The dimensionless version of the fundamental equations and the boundary conditions makes use of the following quantities:

$$\bar{x} = \frac{x}{\lambda}, \bar{y} = \frac{y}{l}, \bar{h} = \frac{h}{a}, \bar{t} = \frac{ct}{\lambda}, \bar{\xi} = \frac{\xi}{a}, \bar{\psi} = \frac{\psi}{ac}, \bar{q} = \frac{q}{ac}, \bar{u} = \frac{u}{ac}, \bar{D}a = \frac{Da}{a^2}, \bar{b} = \frac{b\lambda}{a}, \bar{l} = \frac{l}{a}, \bar{\tau}_0 = \frac{a\tau_0}{\mu c^n} \tag{3}$$

After eliminating the prime elements, the governing equations of motion look like this:

$$-\frac{\partial p}{\partial x} + \eta \sin \theta = \frac{\partial}{\partial y} (\tau) \tag{4}$$

$$(\tau_{yx})^{1/2} = \left( -\frac{\partial u}{\partial y} \right)^{1/2} + \tau_0^{1/2} \tag{5}$$

also, the limits are

$$\psi = 0 \text{ at } y = 0 \quad (6)$$

$$\psi_{yy} = 0 \text{ at } y = 0 \quad (7)$$

$$\tau_{yx} = 0 \text{ at } y = 0 \quad (8)$$

$$u = \psi_y = -\frac{\sqrt{Da}}{\alpha} \frac{\partial u}{\partial y} - 1 \text{ at } y = h(x) - \epsilon \quad (9)$$

$$\text{Where } h(x) = 1 + bx + d\sin 2\pi x \quad (10)$$

## RESOLVING THE ISSUE

By solving Equations (4) and (5) inside the bounds (6) through (9), we obtain the velocity field.

$$u = \frac{P}{2} \left[ \{(h-\epsilon)^2 - y^2\} + 2y_0(h-\epsilon - y) + \frac{8}{3}\sqrt{y_0}\{y^{3/2} - (h-\epsilon)^{3/2}\} + \frac{2\sqrt{Da}}{\alpha}\{(h-\epsilon) - y_0 + 2\sqrt{y_0}(h-\epsilon)^{1/2}\} \right] - 1 \quad (11)$$

$$\text{Where } P = -\frac{\partial p}{\partial x} + \eta \sin \theta \quad (12)$$

If we take the boundary condition at the plug flow region, we get the top limit at  $y_0 = \frac{\tau_0}{P}$

$$\psi_{yy} = 0 \text{ at } y = y_0$$

Using  $y = y_0$  in equation (11) yields the velocity in the plug flow zone,

$$u_p = \frac{P}{2} \left[ (h-\epsilon)^2 + 2y_0(h-\epsilon) - \frac{y_0^2}{3} - \frac{8}{3}(h-\epsilon)^{3/2}y_0^{1/2} + \frac{2\sqrt{Da}}{\alpha}\{(h-\epsilon) - y_0 + 2\sqrt{y_0}(h-\epsilon)^{1/2}\} \right] - 1 \quad (13)$$

The stream functions are obtained by integrating Equations (11) and (13) with  $\psi = 0, y = 0$  and  $\psi = \psi_p$  at  $y = y_0$

$$\psi = \frac{P}{2} \left[ (h-\epsilon)^2 y - \frac{y^3}{3} + 2y_0 \left\{ (h-\epsilon)y - \frac{y^2}{2} \right\} + \frac{8}{3}\sqrt{y_0} \left\{ \frac{2}{5}y^{5/2} - (h-\epsilon)^{3/2}y \right\} + \frac{2\sqrt{Da}}{\alpha}\{(h-\epsilon) - y_0 + 2\sqrt{y_0}(h-\epsilon)^{1/2}\}y \right] - y; \quad y_0 \leq y \leq h \quad (14)$$

To be more precise, the stream function is defined as:

$$\psi_p = \frac{P}{2} \left[ (h-\epsilon)^2 y_0 + 2y_0^2(h-\epsilon) - \frac{y_0^3}{3} - \frac{8}{3}(h-\epsilon)^{3/2}y_0^{3/2} + \frac{2\sqrt{Da}}{\alpha}\{(h-\epsilon)y_0 - y_0^2 + 2y_0^{3/2}(h-\epsilon)^{1/2}\} \right] - y_0 \quad (15)$$

The q-valued volume flux across each cross section is calculated as

$$q = \int_0^{y_0} u_p dy + \int_{y_0}^{h-\epsilon} u dy \quad (16)$$

$$q = \frac{P}{2} \left[ \left\{ \frac{2}{3}(h-\epsilon)^3 \right\} + (h-\epsilon)^2 y_0 - \frac{8}{5}\sqrt{y_0}(h-\epsilon)^{5/2} - \frac{1}{15}y_0^3 + \frac{\sqrt{Da}}{\alpha} \left\{ 2(h-\epsilon)^2 - 2y_0(h-\epsilon) + 4\sqrt{y_0}(h-\epsilon)^{3/2} \right\} - (h-\epsilon) \right] \quad (17)$$

This is deduced from Equations (12) and (17)

$$\frac{\partial p}{\partial x} = -P + \eta \sin \theta = -\frac{30\alpha(q+h-\epsilon)}{(h-\epsilon)^2[(h-\epsilon)+15\tau\alpha(h-\epsilon)-24\sqrt{\tau\alpha}(h-\epsilon)-\tau^3\alpha(h-\epsilon)+45\sqrt{Da}(1-\tau+2\sqrt{\tau})]} + \eta \sin \theta \quad (18)$$

$\bar{Q}$  as is the average volumetric flow rate throughout time

$$\bar{Q} = \frac{1}{T} \int_0^T Q dt = q + 1 \quad (19)$$

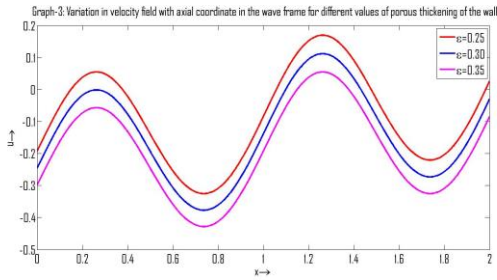
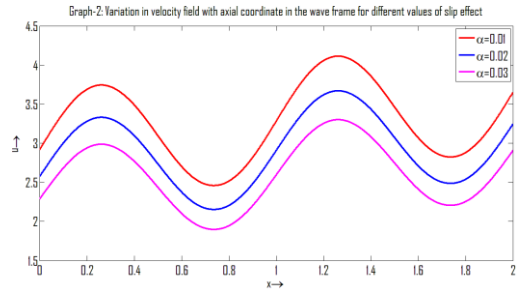
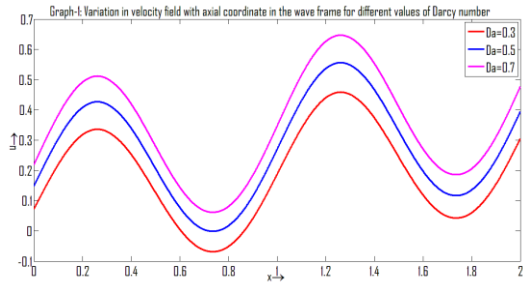
The pressure difference over one wave cycle is provided by the following when equation (18) is integrated over one wavelength:

$$\Delta P = \int_0^1 \frac{\partial p}{\partial x} dx \quad (20)$$

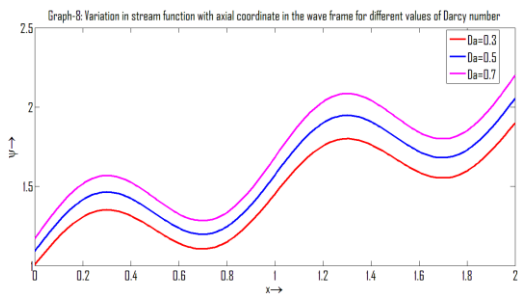
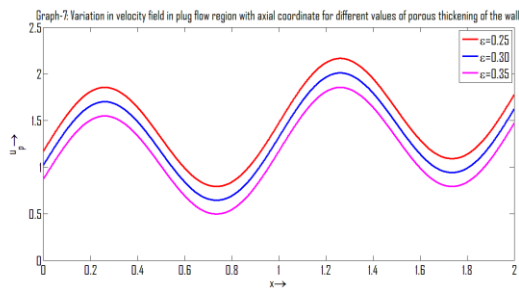
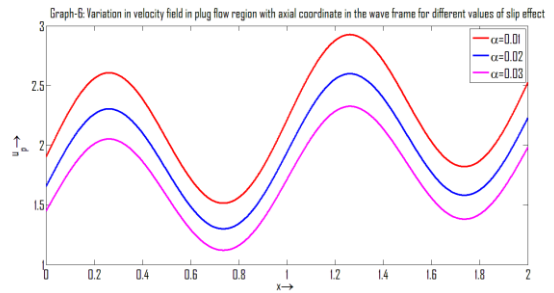
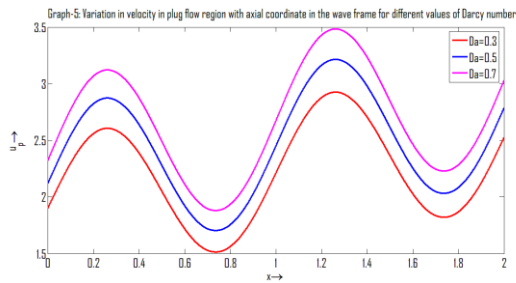
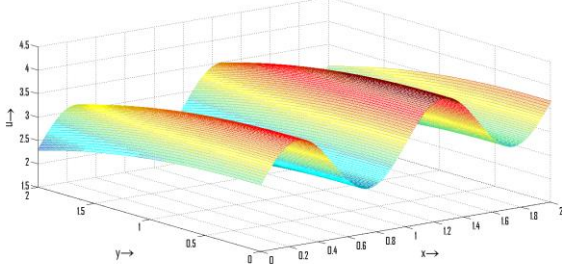
The frictional force  $F$  exerted on the wall during a period of one wavelength is equal to

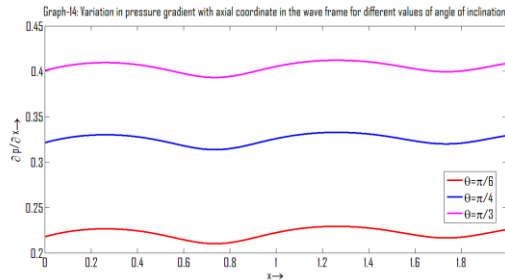
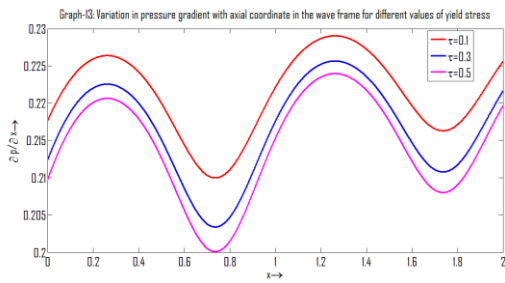
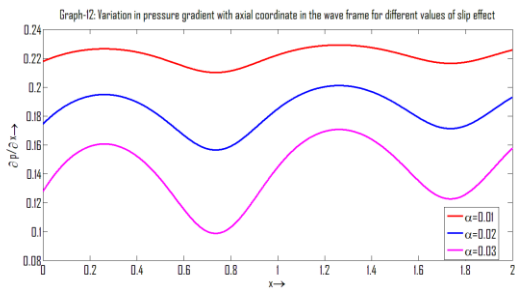
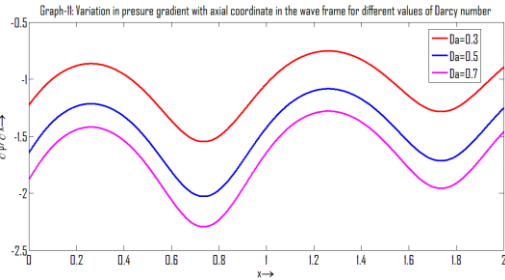
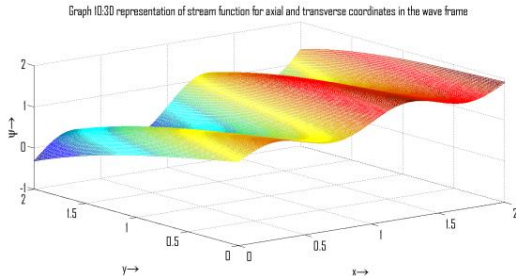
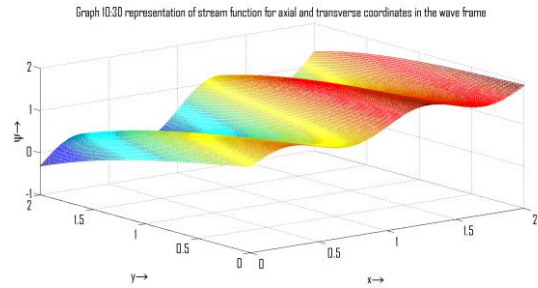
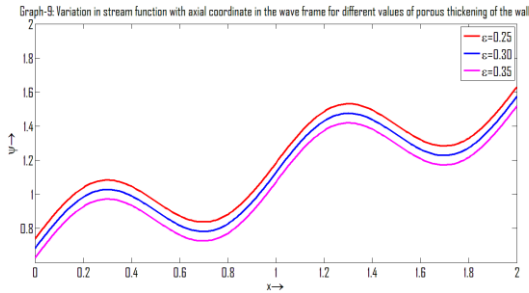
$$F = \int_0^1 h \left( -\frac{\partial p}{\partial x} \right) dx \quad (21)$$

**OUTCOMES AND ANALYSIS**



Graph 4.3D representation of velocity field for axial and transverse coordinates in the wave frame





Equation (11) is used to generate MATLAB graphs for the velocity field versus axial displacement for varying values of the Darcy number, slip effects, and porous thickening of the wall (see graphs 1–3). It is measured, the higher the Darcy number, the higher the velocity and falls with a drop in the slip effect and the porous thickening. Axially and transversely displaced three-dimensional plots of the velocity field are presented in graph (4). For Equation (13), how fast things are moving in the centre of a plug is shown against axial displacement for varying Darcy numbers, slip effects, and porous thickness of the wall in Graphs (5) through (7). The velocity in the plug flow zone is observed to increase with the Darcy number and to decrease with the slip effect and porous thickening. Equation (14) is used to depict stream function vs axial displacement for a range of Darcy numbers and wall porosities in graphs (8) and (9). Increasing the Darcy number and decreasing the thickness of the porous medium are both found to

increase the stream function. Graphs of the stream function in three dimensions, including axial and transverse displacement, are shown in graph (10).

Using Equation (18), we depict the pressure gradient versus axial displacement as a function of the Darcy number, slip effect, yield stress, and wall inclination angle in Graphs (11) and (14). We find that when the Darcy number, slip effect, porous thickness, and yield stress all rise, the pressure gradient falls, but as the angle of inclination rises, the pressure gradient rises.

## CONCLUDING REMARKS

We examine the peristaltic flow of Casson fluid in a non-uniformly inclined channel using a wave frame of reference that travels along with the wave's speed. Taking into account a long wavelength and a small Reynolds number, the model is resolved. The stream function and volume flux at each cross section, as well as the axial velocity and plug flow velocity, are solved for as a function of the axial distance. All of the graphs are made with MATLAB. The following are the results of this study:

- (i) As the Darcy number rises, the velocity field and the velocity in plug flow rise, whereas the performance measures fall as the slip effect and porous thickening fall.
- (ii) Since the Darcy number slip effect, porous thickening, and yield stress all increase as the angle of inclination rises, the pressure gradient decreases.

## REFERENCES

1. Akbar N. S., Butt, A. (2015): "Heat transfer analysis for the peristaltic flow of Herschel Bulkley fluid in a non-uniform inclined channel", *Zeitschrift für Naturforschung Online*, 70 (1):23–32.
2. Ali Abbas M., Bai Y. D., Bhatti M. M., Rashidi M. M. (2016): "Three dimensional peristaltic flow of hyperbolic tangent fluid in non-uniform channel having flexible walls", *Alexandria Engineering Journal*, 55(1):653–662.
3. Gudekote M., Choudhari R. (2018): "Slip Effects on Peristaltic Transport of Casson Fluid in an Inclined Elastic Tube with Porous Walls", *Journal of Advanced Research in Fluid Mechanics and Thermal Sciences*, 43(1): 67-80.
4. Hasan M.M., Samad M.M., Hossain M.M. (2019): "Peristaltic Flow of Non-Newtonian Fluid with Slip Effects: Analytic and Numerical Solutions", *Research Journal of Mathematics and Statistics*, 11(1):1-10.
5. Hummady L.Z., Abdulhadi A.M. (2014): "Effect of heat transfer on the peristaltic transport of MHD with couple-stress fluid through a porous medium with slip effect", *Mathematical Theory and Modeling*, 4 (7):1–18.
6. Laidoudi H., Makinde O.D. (2021): "Computational study of thermal buoyancy from two confined cylinders within a square enclosure with single inlet and outlet ports", *Heat Transfer*, 50(2):1335-1350.
7. Majeed A.H., Mahmood R., Shahzad H., Pasha A.A., Raizah Z.A., Hosham H.A., Reddy D.S.A, Hafeez M.A. (2023): "Heat and mass transfer characteristics in MHD Casson fluid flow over a cylinder in a wavy channel: Higher-order FEM computations", *Case Studies in Thermal Engineering*, 42:102730.
8. Raju K.K., Devanathan, R. (1972): "Peristaltic motion of a non-Newtonian fluid", *Rheologica Acta.*, 11:170–179.
9. Rubinow S. I., Joseph B. Keller. (1972): "Flow of a viscous fluid through an elastic tube with applications to blood flow." *Journal of theoretical biology*, 35(2):299-313.
10. Sankad G.C., Patil A. (2016): "Impact of permeable lining of the wall on the peristaltic flow of Herschel Bulkley fluid", *Applications and Applied Mathematics*, 11(2):663-679.